Surface structure and composition of the alloy $Au_3Pd(100)$ determined by LEED and ion scattering spectroscopy

J. Kuntze, S. Speller, and W. Heiland
Universität Osnabrück, FB Physik, D-49069 Osnabrück, Germany

A. Atrei
Dipartimento di Scienze e Tecnologie Chimiche e dei Biosistemi, Universtità di Siena, 53100 Siena, Italy

G. Rovida and U. Bardi
Dipartimento di Chimica, Università di Firenze, 50121 Firenze, Italy
(Received 16 February 1999)

The (100) surface of the alloy Au_3Pd has been investigated by crystallographic LEED and ion scattering spectroscopy to determine the structure and composition of the first three atomic layers. The observed LEED pattern corresponds to the bulk truncated structure of the substitutionally disordered Au_3Pd alloy. No significant relaxations of the first three layers have been found. Surface segregation of Au has been found by both methods, indicating pure Au in the topmost layer. The second layer is slightly depleted in Au ($c_{Au,2}=0.6 \pm 0.2$). [S0163-1829(99)04428-8]

I. INTRODUCTION

The study of metal-alloy surfaces has gained increasing interest in recent years. Surface segregation and ordering phenomena have often been observed. For Au containing alloys like $Cu_3Au(110)$,[1] $Cu_3Au(100)$,[1,2] $Au_3Cu(100)$,[3] and $Au_3Pd(113)$ (Ref. 4) Au segregates always to the surface. In a previous paper,[5] we described mainly scanning tunneling microscopy (STM), x-ray diffraction (XRD), and noble gas impact collision ion scattering spectroscopy with neutral detection (NICISS) results obtained for $Au_3Pd(100)$. The present paper describes in more detail our low-energy electron diffraction (LEED) and ion scattering (ISS) experiments on this surface, which have only briefly been sketched in the previous paper.

II. EXPERIMENT

The experiments were performed in a vacuum chamber with base pressures in the 10^{-8} Pa range. The chamber was equipped with a hemispherical electron analyzer (modified for the detection of ions) and two-grid optics for LEED. ISS spectra were taken with 1-keV He or Ne with sample currents of 25–30 nA. The scattering angle was 135° and the incidence angle was 45°. The beam was rastered over a 3 mm $\times$ 3 mm area.

The LEED intensity (I-V) curves were measured using a video LEED system in an energy range from 50–400 eV. The I-V curves were acquired for four sets of nonequivalent beams [(1,0), (1,1), (2,0), and (2,1)] at normal incidence of the primary electron beam. The I-V curves for the symmetrically equivalent beams were averaged in order to compensate for the residual minor discrepancies in the normal incidence condition. Intensities were normalized to constant incident current, and the background was estimated from measurements of the intensity in proximity of the spots and subtracted from the I-V curves.

III. CALCULATION METHOD

Dynamical calculations of the LEED intensities were performed using the Barbieri/Van Hove Symmetrized Automated Tensor LEED package.[6] The scattering by Au and Pd atoms was described using eleven phase shifts, derived from a muffin-tin potential calculated for the Au_3Pd alloy using the Barbieri/Van Hove phase-shift package.[7] The bulk Debye temperatures for Au and Pd used in the calculations were 165 and 274 K, respectively.[8] Calculations using an enhanced vibrational amplitude at the surface did not improve the fits and have been omitted. The average-t-matrix approximation[9] was used to calculate the effect of random enrichment in one of the components. The real part of the inner potential was set to 10 V and optimized in the R-factor analysis. The imaginary part of the inner potential was set to 5 V. The calculations were performed in an energy range from 80–380 eV. The calculations were performed for a grid of compositions of the first three layers using the bulk truncated structure of the alloy as reference structure. For each composition, the first three interlayer distances were then optimized in the second step of the TLEED calculations[6] to get the best agreement with the experimental I-V curves. In the R-factor analysis the R_P (Pendry) and R_{MZJ} (modified Zanazzi-Jona) reliability factors[10] and an average of the two were used. The total energy range used in the calculations was 922 eV, and the error bars for the values of the structural parameters were estimated from the variance of the R_P factor,[11] using the formula $\Delta R = R_{min}(8V_{0i}/\Delta E)^{1/2}$, where R_{min} is the minimum of the R_P, V_{0i} is the imaginary part of the inner potential, and ΔE is the total-energy range. The error bars for the layer composition were estimated in the same way, holding all structural parameters and the compositions of the other layers at best-fit values.

IV. RESULTS

After several cleaning cycles using 1-keV Ar^+ followed by annealing to 770 K for 10 min, no contaminants could be

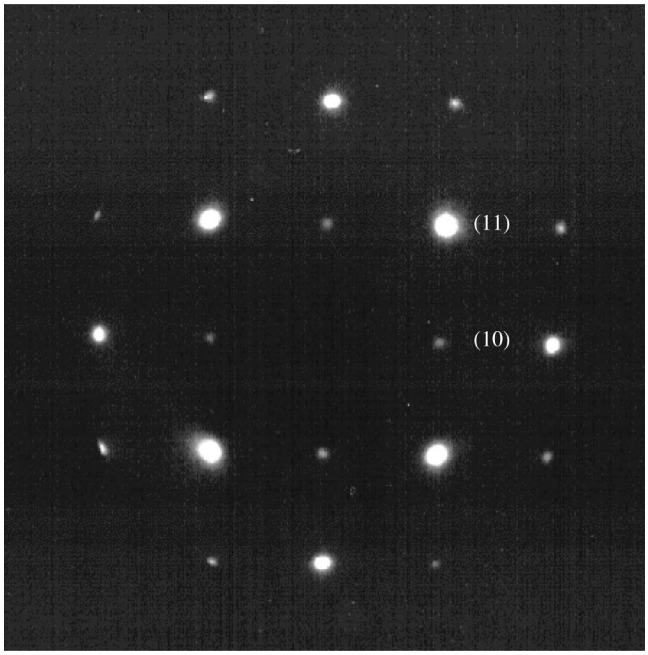

FIG. 1. LEED pattern taken at 142 eV. No superstructure spots can be observed. The spot distances indicate a (1×1) pattern.

detected by x-ray photoemission spectroscopy (XPS) and ISS. The LEED pattern (Fig. 1) shows a sharp (1×1)unit cell. The side of the unit cell is, within the accuracy of the measurement, equal to that of the substitutionally disordered $Au_3Pd(100)$ surface. If the alloy was chemically ordered, one should observe the $c(2\times2)$ periodicity (with respect to the pure Au layers).

ISS spectra taken with 1-keV He (Fig. 2) show segregation of Au upon annealing, with only a residual Pd signal for the annealed surface. The Pd signal is equivalent to approximately 4 at. %, taking into account the respective scattering cross sections and assuming equal neutralization probabilities for Au and Pd. Since no elemental standards were available for our experiments, quantification of ISS intensities should be regarded as an approximation only. Using the elemental sensitivity factors of polycrystalline materials[12] for 1 keV He^+ scattering, the Pd-surface concentration is estimated to 6 at. % for the annealed surface and 25 at. % for the sputtered surface, equal to the bulk concentration. The residual Pd signal could be due to a sputtering effect during the time of the measurement (5 min/spectrum).

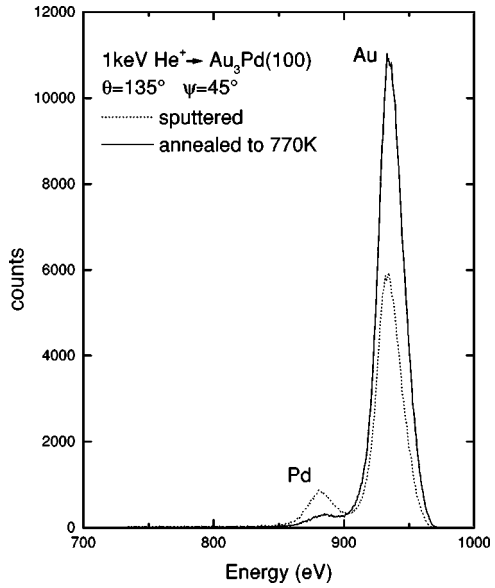

FIG. 2. Low-energy ion scattering spectra taken with 1-keV He^+ after sputtering (dotted line) and annealing to 770 K (solid line).

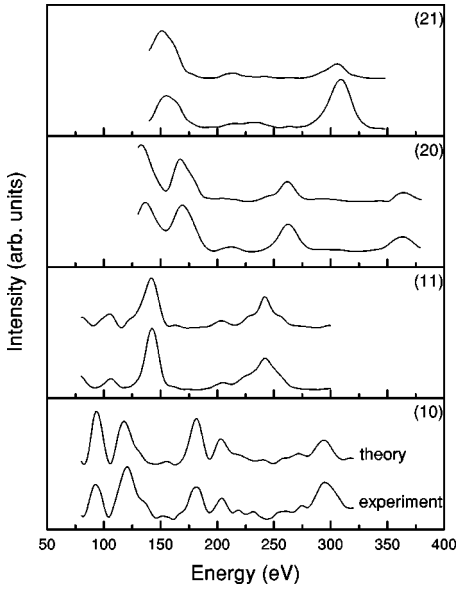

FIG. 3. Comparison between experimental and calculated I-V curves. All data are acquired at normal incidence. The calculated curves correspond to the minimum of the *R*-factor analysis.

For the LEED calculations, a grid of compositions has been tested: the Au concentration, as atomic fraction, in the first two atomic layers has been varied from 0–1 in steps of 0.2, with bulk concentration in all deeper layers. Best agreement was achieved with $c_1=1.00$ and $c_2=0.60$ (the index denotes the atomic layer), with $R_P=0.235$ and $R_{MZJ}=0.12$. The first interlayer spacing is contracted by 0.02 Å, the second by 0.03 Å . The third layer shows no relaxation. Variation of the third layer composition did not improve the fit, neither did a variation of the first and second layer composition in proximity of the minimum found in the coarse grid. Additionally the lattice constant was varied, which led to an *R*-factor minimum ($R_P=0.206$, $R_{MZJ}=0.096$) at 3.99 Å. This value is in good agreement with previous NICISS data[5] and an additional LEED data set measured in a different laboratory. However, using the conservative estimation (variance of R_P) for the error bars, the minimum is not clearly significant in our case. So we can't state the contraction of the unit cell on the basis of our data alone, since this would require a larger data set and even better theory-experiment agreement. But taking into account the results of the other experiments, a (numerical) artifact can clearly be excluded. The best fit values for the composition and the first three interlayer spacings did not change upon variation of the lattice constant. The comparison of the experimental and the theoretical curves is shown in Fig. 3. The sensitivity of the R_P factor to the structural parameters and to the composition

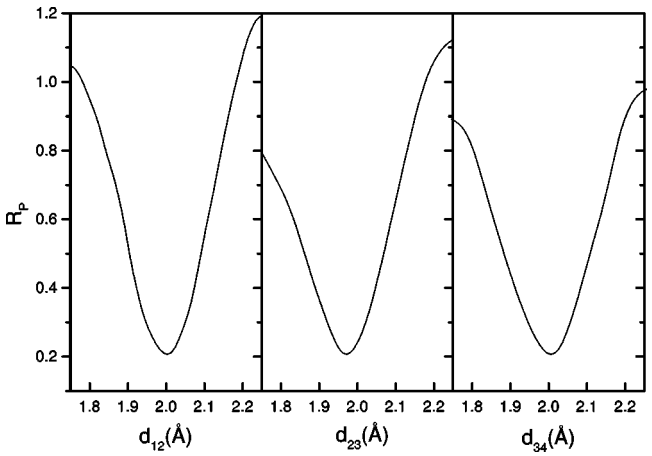

FIG. 4. R_P factor as a function of the structural parameters.

is shown in Figs. 4 and 5, respectively. The final structure and composition is listed in Table I.

V. DISCUSSION

The agreement between theory and experiment is within the limits for a satisfactory structural determination.[10] Both ISS and LEED indicate a first layer consisting of pure Au. As derived by LEED, the second layer is slightly depleted in Au (60 ± 20 at. % instead of 75 at. %). Although the sensitivity to random enrichment in one of the components is quite low, the fact that calculations with different R factors yield the same minimum indicates that the depletion is significant. We note, however, that the bulk composition of 75 at. % is within the error bars of our analysis. We regard the conservative estimate of error bars as appropriate for our data set, although a recent study has shown that the sensitivity for compositional variations may be underestimated by this approach.[13] In order to achieve a much better accuracy (within ±8 at. %), a theory-experiment agreement well below $R_P=0.2$ is required, which was not possible in our case due to residual stray magnetic fields adding noise to the data.

The alloy is substitutionally disordered within the penetration depth of the electrons, and shows a bulk-truncated fcc structure with a lattice parameter of 3.99 ± 0.02 Å . The relaxations found for the first three interlayer spacings are

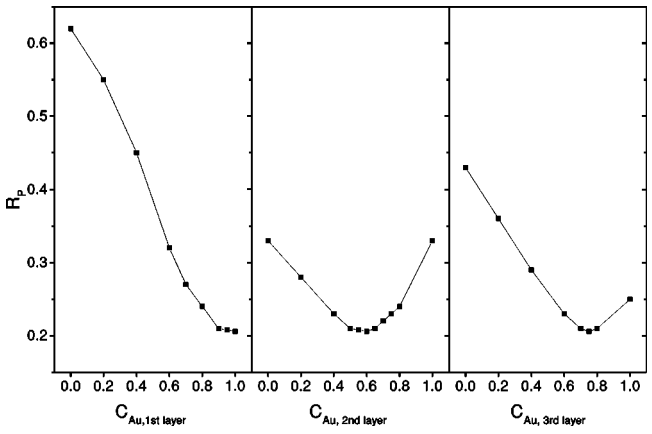

FIG. 5. R_P factor as a function of the composition in the first three layers.

TABLE I. Structure and composition of the first three atomic layers for $Au_3Pd(100)$.

d_{12}	2.00 ± 0.03 Å	$c_{Au,1}$	1.0 ± 0.2
d_{23}	1.97 ± 0.03 Å	$c_{Au,2}$	0.6 ± 0.2
d_{34}	2.01 ± 0.03 Å	$c_{Au,3}$	0.75 ± 0.2
d_{bulk}	1.995 Å	$c_{Au,bulk}$	0.75

within the error bars of the present analysis. Additional experiments using ISS, crystallographic LEED, and STM have been performed in a different laboratory,[5] and confirm the findings reported here.

The question whether the Au_3Pd alloy is chemically ordered or not is still not conclusively discussed in the literature. There is only little data dealing with this question, and only one study has found chemical order.[14] This study has, however, been performed with vapor-deposited Au and Pd films, which have been subsequently annealed for alloying. It has also been noted in that study that no chemical long-range order has been observed in bulk specimen, which was believed to be due to insufficient annealing. Another study[15] failed to reproduce the findings of Ref. 14. Therefore, we tend to conclude that the alloy indeed is substitutionally disordered in the bulk state. This is also corroborated by theoretical studies using an combined embedded atom method/Monte Carlo simulation approach to calculate the order parameter.[16]

The (100) oriented surface of gold is known to be reconstructed in a similar way to the Pt(100) and Ir(100) surfaces.[17,18] For these surfaces the topmost layer reconstructs to a near hexagonal arrangement, leading to a $c(26\times68)$-LEED pattern in the case of Au(100).[17] Despite the fact that $Au_3Pd(100)$ terminates with a layer of (nearly) pure gold, this surface is not reconstructed.

On the other hand, the (100) surfaces of Pt alloys terminating with a layer of pure platinum [see for instance the cases of $Pt_{80}Co_{20}$,[19] $Pt_{50}Ni_{50}$ (Ref. 20)] are reconstructed in a similar way to the Pt(100) surface. In the case of gold the presence of the other metal in the alloy stabilizes the unreconstructed surface. Indeed, the $Au(100)(1\times1)$ surface can be stabilized by deposition of a submonolayer fraction of rhodium as shown by Jona *et al.*[21]

In addition to these chemical causes, the (lateral) lattice constant contraction can be a reason for the nonreconstructed surface. The driving force for the quasihexagonal arrangement is generally believed to be stress, which is relieved by a compression of the toplayer atom spacing. In the case of Au_3Pd, the lattice constant of 3.99 Å is 2.2% smaller than for bulk gold (4.08 Å). This reduction may be the reason why no reconstruction of the topmost layer is found for the alloy, hence $Au_3Pd(100)$ seems to provide the substrate for stress-free growth of a Au(100) monolayer. It would be interesting to grow gold on this substrate and see if (and when) the surface reconstructs.

VI. SUMMARY

The $Au_3Pd(100)$ surface has been investigated by crystallographic (Tensor-) LEED and ISS to determine the structure and composition of the first three atomic layers. The ob-

served LEED pattern corresponds to the substitutionally disordered Au_3Pd alloy, showing no evidence for chemical long-range order. A first layer composition of pure gold has been found with ISS and LEED after annealing to 770 K. The second layer seems to be slightly depleted in Au according to LEED (60 ± 20 at.% Au). The third layer has bulk composition within the error limits of the measurement. The first three interlayer spacings are $d_{12}=2.00\pm0.03$ Å, $d_{23}=1.97\pm0.03$ Å, and $d_{23}=2.01\pm0.03$ Å. Within the error limits, they correspond to the bulk spacing. Unlike pure Au(100), the surface of the alloy is not reconstructed. This may be due to the presence of Pd in the second layer and/or due to a smaller lattice constant of the alloy (3.99 ± 0.02 Å as derived by LEED) compared to bulk Au.

ACKNOWLEDGMENTS

Financial support by the Deutsche Forschungsgemeinschaft (DFG), the Deutsche Akademische Austauschdienst (DAAD, Vigoni-Program), and the ESF is gratefully acknowledged. We thank M. Aschoff (University of Osnabrück) and E. Platzgummer (TU Wien) for providing additional data sets for comparison and discussion.

[1] H. Niehus, Phys. Status Solidi B **192**, 357 (1995).
[2] L. Houssiau and P. Bertrand, Nucl. Instrum. Methods Phys. Res. B **125**, 328 (1997).
[3] S. Schömann and E. Taglauer, Surf. Rev. Lett. **3**, 1823 (1996).
[4] A. Piaszenski, M. Aschoff, S. Speller, and W. Heiland, Nucl. Instrum. Methods Phys. Res. B **135**, 331 (1998).
[5] M. Aschoff, S. Speller, J. Kuntze, W. Heiland, E. Platzgummer, M. Schmid, P. Varga, and B. Baretzky, Surf. Sci. Lett. **415**, L1051 (1998).
[6] A. Barbieri and M.A. Van Hove, *Symmetrized Automated Tensor LEED Package, Version 4.1* (M. A. Van More, Berkeley, CA, 1996) (http://electron.lbl.gov/leedpack/leedpack.html).
[7] A. Barbieri and M. A. Van Hove (private communication).
[8] C. Kittel, *Einführung in die Festkörperphysik*, 9th ed. (Oldenbourg, München, 1991).
[9] S. Crampin and P.J. Rous, Surf. Sci. Lett. **244**, L137 (1991).
[10] M. A. Van Hove, W. H. Weinberg, and C.-M. Chan, *Low-Energy Electron Diffraction*, Springer Series in Surface Sciences, Vol. 6 (Springer-Verlag, Berlin, 1986).
[11] J. B. Pendry, J. Phys. C **13**, 937 (1980).
[12] E. Taglauer, Appl. Phys. A: Solids Surf. **38**, 161 (1985).
[13] M. Sporn, E. Platzgummer, S. Forsthuber, M. Schmid, W. Hofer, and P. Varga, Surf. Sci. **416**, 423 (1998).
[14] A. Nagasawa, Y. Matsuo, and J. Kakinoki, J. Phys. Soc. Jpn. **20**, 1881 (1965).
[15] Y. Kawasaki, S. Ino, and S. Ogawa, J. Phys. Soc. Jpn. **30**, 1758 (1971).
[16] J. Kuntze, P. Deurinck, A. Atrei, U. Bardi, S. Speller, C. Creemers, and W. Heiland (unpublished).
[17] M. A. Van Hove, R. J. Koestner, P. C. Stair, J. P. Bibérian, L. L. Kesmodel, I. Bartoš, and G. A. Somorjai, Surf. Sci. **103**, 189 (1981).
[18] G. Ritz, M. Schmid, P. Varga, A. Borg, and M. Rønning, Phys. Rev. B **56**, 10 518 (1997).
[19] U. Bardi, A. Atrei, E. Zanazzi, G. Rovida, and P.N. Ross, Vacuum **41**, 437 (1990).
[20] Y. Gauthier, R. Baudoing-Savois, J. Rundgren, M. Hammar, and M. Gothelid, Surf. Sci. **327**, 100 (1995).
[21] S. C. Wu, H. Li, J. Quinn, Y. S. Li, A. M. Begley, S. K. Kim, F. Jona, and P. M. Marcus, Phys. Rev. B **49**, 8353 (1994).